

## Studies on Adiabatic Shear Bands of Ti6Al4V after Hot Compression

Xiang-Hong XU<sup>1,2,a</sup>, Yan-Qing YANG<sup>2,b,\*</sup>, Liu-Qing YANG<sup>2,c</sup>

<sup>1</sup>Shazhou Professional Institute of Technology, Zhangjiagang 215600, China

<sup>2</sup>State Key Lab of Solidification Processing, School of Materials Science and Engineering, Northwestern Polytechnical University, Xi'an 710072, China

<sup>a</sup>xxh602@126.com, <sup>b</sup>yqyang@nwpu.edu.cn, <sup>c</sup>441951285@qq.com

\*Corresponding author

**Keywords:** Ti6Al4V, Adiabatic Shear Band, Texture, EBSD.

**Abstract.** The adiabatic shear bands were induced in Ti6Al4V alloy with original equiaxed grain by compressing cylindrical sample with the strain rate of  $50\text{s}^{-1}$  at  $750^\circ\text{C}$  and studied by using electron backscattered diffraction. Three regions of matrix, elongated transition region and ASBs, can be observed in the deformed sample. The matrix mainly contains equiaxed  $\alpha$  grains with  $\{0001\} \langle 10\bar{1}0 \rangle$  texture. Strong  $\{10\bar{1}0\} \langle 11\bar{2}0 \rangle$  texture and  $\{11\bar{2}2\} \langle 11\bar{2}3 \rangle$  texture were identified in the transition region with severe elongated grains about 1-4 $\mu\text{m}$  in width. In the center of ASBs, there exist equiaxed grains of 0.2-0.7 $\mu\text{m}$  in size without orientation focus. However, the ASBs close to the surface of the sample still have highly elongated microstructure exhibiting a  $\{11\bar{2}0\} \langle 10\bar{1}0 \rangle$  type texture component.

### Introduction

Adiabatic shear bands (ASBs) appear in alloys deformed at high strain rates and are characterized by large localized deformation in a narrow band of 5-100 $\mu\text{m}$ <sup>[1]</sup>. ASBs have been observed in many cases such as machine chips, ballistic impact loading shear and so on. Normally, adiabatic shearing is undesirable because the formation of ASBs makes the material to lose its load carrying and energy dissipation capacity and even to be failure<sup>[2]</sup>. On the other hand, recently developed adiabatic cutting and blanking techniques intentionally use the ASBs phenomenon<sup>[3]</sup>.

Ti6Al4V is a widely used titanium alloy. It was found that the ASBs of Ti6Al4V with bimodal microstructure at strain rates of  $10^3$ - $10^4\text{s}^{-1}$  are regularly spaced and orientated along the maximum shear stress plane. While the alloy is with lamellar microstructure, its ASBs go through the transition from self-organization to branching off and interconnecting into a net-like structure<sup>[4]</sup>. The number of ASBs in equiaxed microstructure is larger than that in bimodal one<sup>[5]</sup>. Moreover, adiabatic shear banding of Ti6Al4V turns out to be the major fracture mode when the alloy is deformed to large plastic strain at high temperature and high strain rate<sup>[6]</sup>.

In most previous research on ASBs, the strain rate is higher than  $10^3\text{s}^{-1}$ . However, in this study, the Ti6Al4V alloy was hot compressed with relatively lower strain rate of  $50\text{s}^{-1}$ . The microstructure and texture of ASBs in Ti6Al4V were then investigated. It is meaningful for the hot working of Ti6Al4V pieces in industry.

### Experimental

The as-received Ti6Al4V alloy is with equiaxed microstructure. Cylindrical specimens with 12 mm in height and 8 mm in diameter were compressed by a Gleeble-3500 thermo-mechanical simulator at temperature  $650^\circ\text{C}$  and  $750^\circ\text{C}$  with strain rate  $50\text{s}^{-1}$  and engineering compressive strain 50% and 70%, respectively. In order to reduce friction, a tantalum foil with a thickness of 0.1mm was put between the anvil and the specimen. After hot compressing and water cooling, the specimen was cut parallel to the load axis Z (as shown by the dotted lines in Fig.1(a)). Cracks can be seen in Fig.1(a). The sample was mechanically grounded and polished prior to observation.

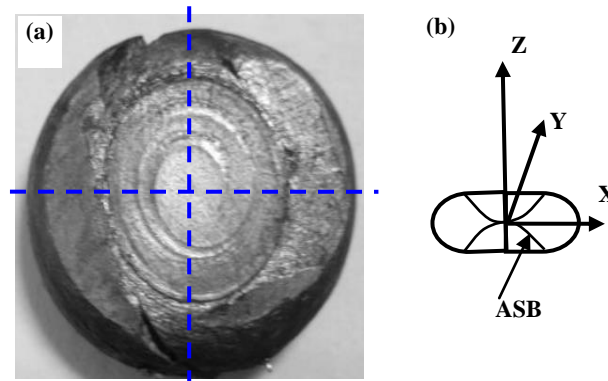


Fig.1 Macro photograph of the Compressed Specimen (a) and Schematic of Longitudinal Section of the Specimen (b)

The microstructure of the deformed specimen was examined respectively by Lasertech C130 confocal microscope and Tescan Mira 3 scanning electron microscope (SEM) with field emission gun after etching the sample. The electron backscattered diffraction (EBSD) analysis for its texture was conducted by using Oxford HKL Nordly Max EBSD accessory installed in the SEM. The sample for EBSD analysis was prepared by electrolytic polishing. As severe deformation of the specimen can cause orientation uncertainty and orientation noise, which possibly leads to blurring of the grain boundaries, misorientations below  $2^\circ$  are not considered in EBSD analysis<sup>[7]</sup>.

## Results and Analysis

It was found that the ASBs can be seen clearly in the specimen compressed under the condition of  $750^\circ\text{C}/50\text{s}^{-1}/70\%$ , as shown in Fig.2. Therefore, following analysis is on this one.

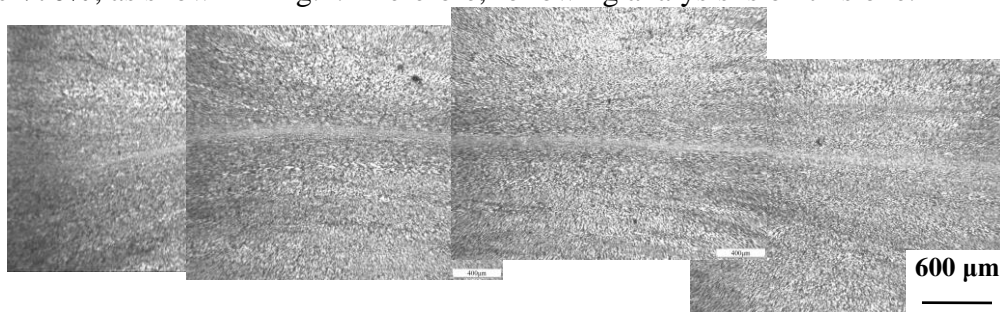


Fig.2 Optical Metallograph in *Y-Z* Plane of the Specimen Deformed at  $750^\circ\text{C}/50\text{s}^{-1}/70\%$

The microstructure in *Y-Z* plane and in *X-Z* plane of the specimen was observed. Fig. 2 is the optical metallograph of *Y-Z* plane as indicated in Fig.1(b). The white ASB is nearly flat and normal to the load axis *Z* in the centre part of the sample. But it turns to its shearing direction on the top and bottom edges. SEM image in Fig.3 shows the microstructure of ASBs close to the bottom edge of the sample in *X-Z* plane. A, B and C in the image are the matrix, transition region and ASBs, respectively. The matrix A is with equiaxed and elongated grains of about  $20\mu\text{m}$  in size. B is the transition region with severely elongated microstructure turning to the shear direction gradually. C shows fiber-like microstructure of ASBs with blurred grains. The three regions are the typical feature of ASBs as observed in specimens deformed by Split Hopkinson Pressure Bar, Ballistic Impact Test, and so on<sup>[8-10]</sup>. It was observed that a lot of voids exist in the interface between ASBs and matrix material and the voids even grow up and merge into a long void along adiabatic shear band, and then these long voids grow into a macrocrack<sup>[4]</sup>. This may be the reason of the cracking as shown in Fig.1(a). However, in our observation, voids cannot be found due to the cutting position.

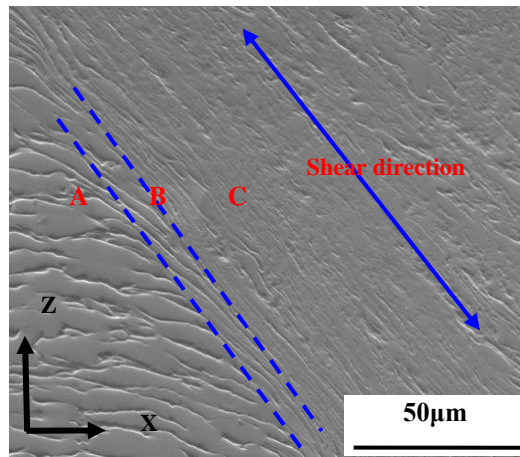


Fig.3 SEM Image of ASBs. (A: matrix, B: transition region, C: ASBs)

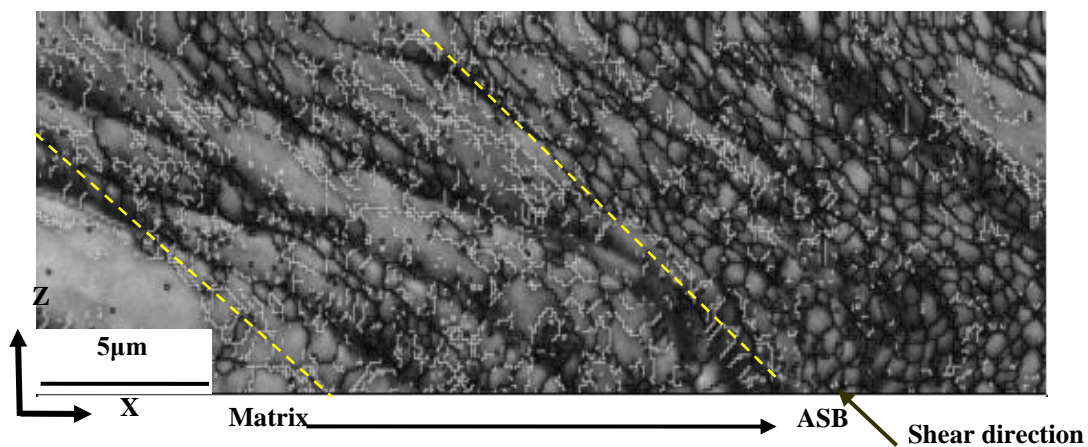


Fig.4 Band Contrast Image of Matrix, Transition and ASBs (Black Lines: HAGBs; Grey Lines: LAGBs)

The grains of ASBs are blurred in SEM photographs. But EBSD analysis can show them clearly. Fig.4 is an EBSD band contrast image of the transition region and ASBs, showing the grains and misorientations. It is obviously that, in the transition region, there are numbers of low angle grain boundaries (LAGBs, grey lines) and some of high angle grain boundaries (HAGBs, black lines). In the ASBs, high angle grain boundaries are dominated. Namely there exist a lot of newly formed equiaxed grains. More details can be found in Fig.5. The matrix in Fig.5(a) contains equiaxed  $\alpha$  grains and intergranular  $\beta$  phase (indicated by arrows) in small amounts. In the transition region, as shown in Fig.5(b), highly elongated grains of about 1-4µm in width are observed with some subgrains inside. The closer to the ASBs is, the thinner the grains are. And no substructure can be seen in the small amount of elongated intergranular  $\beta$  phase, as indicated by arrows. Fig.5(c) shows nearly all the equiaxed grains with HAGBs (black lines) in the center of ASBs. The size of equiaxed grains with much lower dislocation density is about 0.2-0.7µm. Evidently characteristics of large numbers of small grains presented in the center of ASBs are caused by dynamical recrystallization during the adiabatic shearing. Fig.5(d) shows the ASBs close to the surface of the specimen. Compared with that in Fig.5(c), due to the incomplete recrystallization, there are highly elongated subgrains in Fig5(d), even though large numbers of small grains exist. Furthermore, the grain size in Fig.5(d) is smaller than that in Fig.5(c), which means that the recrystallization in the center of ASBs is more perfect due to the more severe strain and so the larger deformation heat.

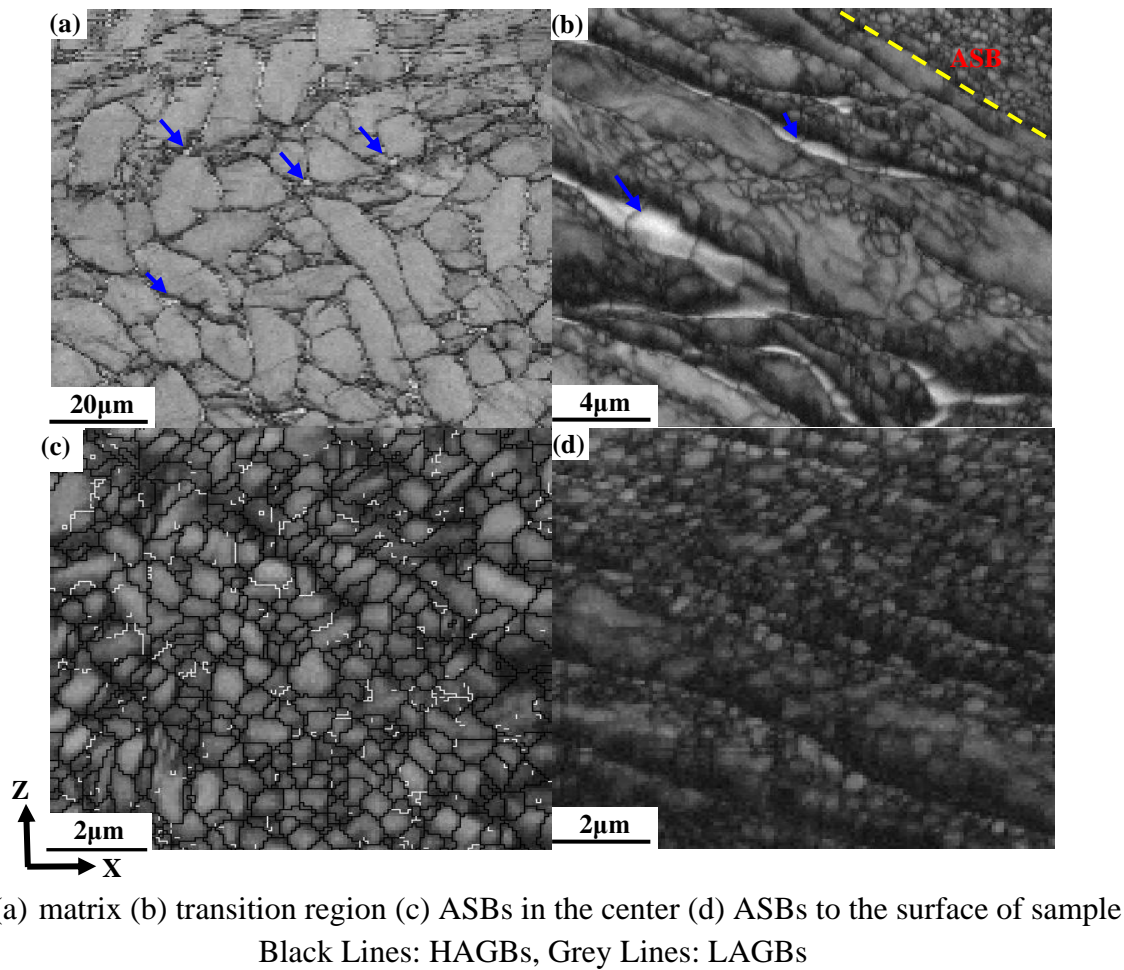
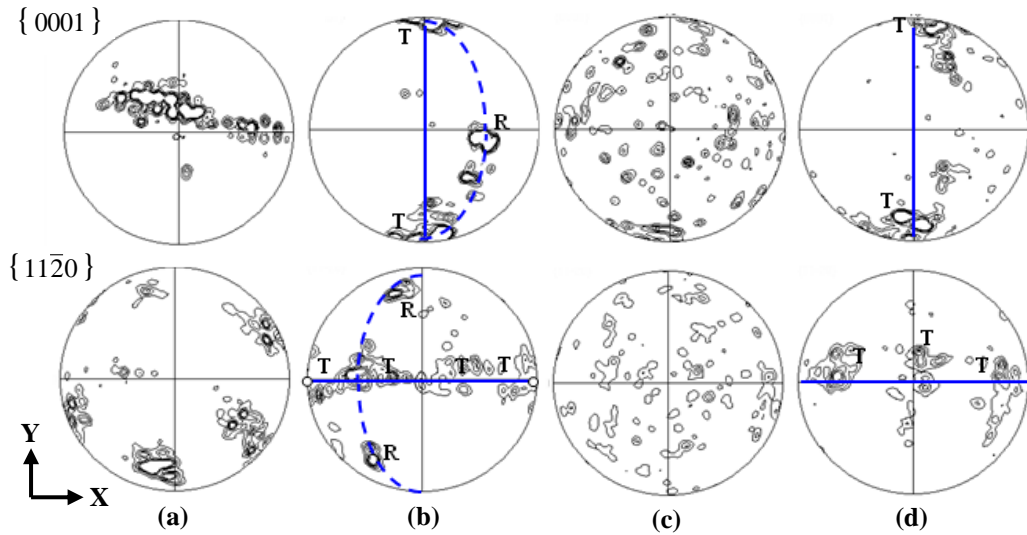


Fig.5 Band Contrast Images of Different Regions

The microstructure evolution in the ASBs can be concluded as subgrain rotation and dynamic recrystallization which was first proposed by Nesterenko<sup>[11]</sup>. At the initial stage of deformation, due to the interaction of compressing and shearing, grains are elongated to the shear direction. At the same time there are random dislocations in the grains. As intensity of the dislocations increase, the elongated dislocation cells form. As deformation proceeds, dislocation cells absorb dislocation, at the same time the misorientation of dislocation cells increase, and then dislocation cells grow into subgrains. In order to adapt deformation, subgrains break and form new subgrains with smaller size. Finally through subgrains rotation, the recrystallized grains form.

Fig.6 shows the pole figures of  $\alpha$  grains in different regions corresponding to Fig.5. Fig.6(a) shows strong  $\{0001\} \langle 10\bar{1}0 \rangle$  texture in the matrix. For the transition region, Fig.6(b) indicates strong  $\{10\bar{1}0\} \langle 11\bar{2}0 \rangle$  texture (marked with T) with the c-axis of the hcp  $\alpha$  crystallites lying within the X-Y plane, and  $\{11\bar{2}2\} \langle 11\bar{2}3 \rangle$  texture (marked with R)<sup>[12]</sup> oriented to the shear direction. The pole figures of the ASBs in the center (Fig.6(c)) reveal nearly no preferred orientation. It confirms that the small grains as shown in Fig.5(c) are newly formed by recrystallization. ASBs close to the surface of the specimen (Fig.6(d)) exhibits a  $\{11\bar{2}0\} \langle 10\bar{1}0 \rangle$  type texture component. Fig.7 is a sketch map of the orientation of the matrix, transition region and ASBs in the center and close to the surface, corresponding to Fig.5 and Fig.6, which shows the distribution of texture more clearly.



(a) Matrix (b) Transition Region (c) ASBs in the Center (d) ASBs to the Surface of Sample

Fig.6 Pole Figures of  $\alpha$  Phase in Different Regions

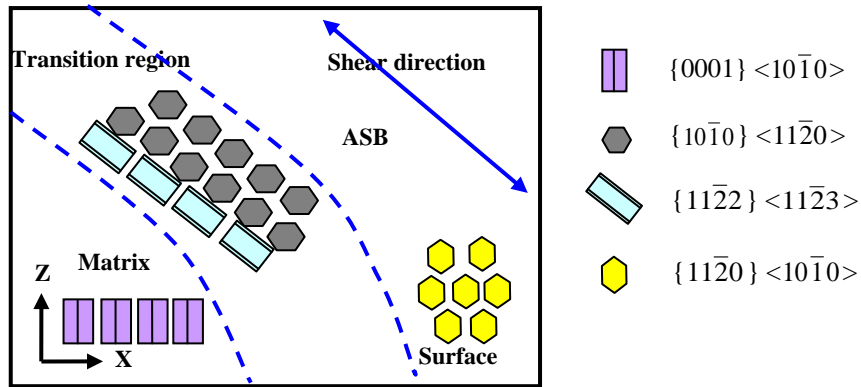


Fig.7 Sketch Map of the Orientation in Different Regions

## Summary

Three regions in the Ti6Al4V with original equiaxed microstructure can be identified after compressing at 750°C with strain rate of 50s<sup>-1</sup> for engineering strain of 70%. The matrix contains mainly equiaxed and elongated  $\alpha$  grains of about 20 $\mu$ m in size, exhibiting strong {0001} <10 $\bar{1}$ 0> texture. In the transition region, severely elongated  $\alpha$  grains of about 1-4 $\mu$ m in width with some subgrains inside are observed and there are strong {10 $\bar{1}$ 0} <11 $\bar{2}$ 0> texture and {11 $\bar{2}$ 2} <11 $\bar{2}$ 3> texture. The adiabatic shear bands can be divided into two parts. In the center of adiabatic shear bands, equiaxed grains of 0.2-0.7 $\mu$ m in size, with nearly no preferred orientation, are formed by dynamical recrystallization. The adiabatic shear bands close to the surface of the specimen still reveal elongated microstructure with {11 $\bar{2}$ 0} <10 $\bar{1}$ 0> texture, although there exist a lot of new grains with smaller grain size than that in the center of adiabatic shear bands.

## Acknowledgement

This research was financially supported by the Natural Science Foundation of China (51071122, 51271147), the 111 Project of China (B08040) and The 2015 professional construction engineering education projects of Jiangsu Province (PPZY2015B184).

## References

- [1] Y. Bai, B. Dodd, *Adiabatic shear localization: occurrence, theories and applications*, Pergamon Press, New York, 1992.
- [2] J. Peirs, P. Verleysen, J. Degrieck, F. Coghe. The use of hat-shaped specimens to study the high strain rate shear behaviour of Ti-6Al-4V. *Int. J. Impact Eng.* 37 (2010) 703-714.
- [3] J. Peirs, W. Tirry, F. Coghe, P. Verleysen, L. Rabet, D. Schryvers, J. Degrieck, Microstructure of adiabatic shear bands in Ti6Al4V, *Mater. Charact.* 75 (2013) 79-92.
- [4] X.Q. Liu , C.W. Tan, J. Zhang, Y.G. Hu, H.L. Ma, F.C. Wang, H.N. Cai. Influence of microstructure and strain rate on adiabatic shearing behavior in Ti-6Al-4V alloys, *Mater. Sci. Eng. A*, 501 (2009) 30-36.
- [5] D.G. Lee, Y.H. Lee, S. Lee, Dynamic deformation behavior and ballistic impact properties of Ti-6Al-4V alloy having equiaxed and bimodal microstructures, *Metall. Mater. Trans. A*, 35 (2004) 3103-3112.
- [6] W.S. Lee, C.F. Lin, Plastic deformation and fracture behaviour of Ti-6Al-4V alloy loaded with high strain rate under various temperatures, *Mater. Sc. Eng. A*, 241(1998) 48-59.
- [7] Z.P. Zeng, S. Jonsson, H.J. Roven, The effects of deformation conditions on microstructure and texture of commercially pure Ti, *Acta Mater.* 57 (2009) 5822-5833.
- [8] F. Martinez, L.E. Murr, A. Ramirez, M.I. Lopez, S.M. Gaytan, Dynamic deformation and adiabatic shear microstructures associated with ballistic plug formation and fracture in Ti-6Al-4V targets, *Mater. Sci. Eng. A*, 454 (2007) 581-589.
- [9] B.F. Wang, Y. Yang, Microstructure evolution in adiabatic shear band in fine-grain-sized Ti-3Al-5Mo-4.5V alloy, *Mater. Sci. Eng. A*, 473 (2008) 306-311.
- [10] D. Yang, Y. An, P. Cizek, P. Hodgson, Development of adiabatic shear band in cold-rolled titanium, *Mater. Sci. Eng. A*, 528 (2011) 3990-3997.
- [11] V.F. Nesterenko, M.A. Meyers, J.C. La Salvia, Shear location and recrystallization in high-strain, high-strain-rate deformation of tantalum. *Mater. Sci. Eng. A*, 229 (1997) 23-41.
- [12] M. Karadge, M. Preuss, C. Lovell, P.J. Withers, S. Bray, Texture development in Ti-6Al-4V linear friction welds, *Mater. Sci. Eng. A*, 459 (2007) 182-191.